3. M. A. Gol'dshtik and V. N. Shtern, Hydrodynamic Stability and Turbulence [in Russian], Nauka, Novosibirsk (1977).
4. C. Nakaya, "Three-dimensional waves in boundary layer," in: Laminar-Turbulent Transition: Symp., Stuttgart (1979); Berlin e.a. (1980).
5. D. J. Benny and C. C. Lin, "On the secondary motion induced by oscillations in a shear flow," Phys. Fluids, 3, No. 4 (1960).
6. D. J. Benny, "Finite amplitude effects in an unstable laminar boundary layer," Phys. Fluids, 7, No. 3 (1964).
7. B. N. Antar and F. G. Collins, "Numerical calculation of finite amplitude effects in unstable laminar boundary layers," Phys. Fluids, 18, No. 3 (1975).
8. N. A. Zheltukhin and N. M. Terekhova, "Secondary flows in unstable boundary layers," Zh. Prikl. Mekh. Tekh. Fiz., No. 4 (1981).
9. R. Betchov and W. O. Criminale, Jr., Stability of Parallel Flows, Academic Press (1967).
10. V. N. Zhigulev, "Nonlinear theory of disturbance growth," in: Aerodynamics and Physical Kinetics [in Russian], Inst. Theoretical and Applied Mechanics, Siberian Branch, Academy of Sciences of the USSR, Novosibirsk (1977).
11. S. A. Gaponov and B. Yu. Skobelev, "Secondary similarity conditions for Blasius flow," in: Problems in Hydrodynamics [in Russian], Institute of Theoretical and Applied Mechanics, Siberian Branch, Academy of Sciences of the USSR, Novosibirsk (1975).
12. P. S. Klebanoff, K. D. Tidstrom, and L. M. Sargent, "The three-dimensional nature of boundary-layer instability," J. Fluid Mech., 12, Pt. 1 (1962).
13. N. N. Yanenko, The Method of Fractional Steps in the Solution of Multivariable Problems in Mathematical Physics [in Russian], Nauka, Novosibirsk (1967).

THERMAL CONVECTION IN A HORIZONTAL LAYER WITH LATERAL HEATING

A. G. Kurdyashkin, V. I. Polezhaev, and A. I. Fedyushkin

UDC 536.252+532.5+532.68

1. Introduction. We consider convection in a horizontal layer in a uniform gravitational field with a thermal gradient directed along the layer. Along with the well-known Rayleigh—Benard problem on the convection in a layer heated from below, this one of the fundamental problems in the theory of thermal convection. Recently, there has been interest in this problem because of new experimental techniques, and various engineering and geophysical applications (transport processes during crystallization, in solar collectors, in shallow reservoirs, etc.). Because the state of hydrostatic equilibrium does not exist, unlike the case of heating from below, here convection is induced for any nonzero horizontal temperature difference. However, the intensity of convection and its effect on the temperature (or concentration) field depends significantly on the length-to-width ratio of the layer, and the Rayleigh and Prandtl numbers. An essential role is played by the heat-exchange conditions at the upper and lower horizontal surfaces; these conditions vary widely in practice. Thus, there are a large number of different multiparameter convective processes whose study requires a mathematical model based on the Navier—Stokes equations, and a test of the adequacy of the model by comparison with experiment.

The case most studied theoretically is the situation where identical (linear) temperature distributions are given along both horizontal boundaries. Several papers have considered the flow stability in this case for an infinitely long layer [1, 2]. Convection leads to an unstable vertical temperature distribution at the lower and upper boundaries of the layer.

In the present paper, we experimentally and theoretically study another case, where the horizontal boundaries of the layer are thermally insulated, and different temperatures are specified on the lateral walls. Then convection always leads to an unstable vertical temperature distribution, and this essentially changes the flow structure and heat transport. A

Translated from Zhurnal Prikladnoi Mekhaniki i Tekhnicheskoi Fiziki, No. 6, pp. 122-128, November-December, 1983. Original article submitted October 10, 1982.

 0021-8944/83/2406-0876$07.50 © 1984 Plenum Publishing Corporation

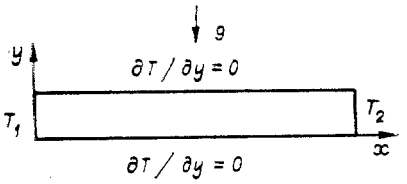

Fig. 1

considerable number of papers in recent years have considered this type of problem [2-13]. The early results [2-4] demonstrated a stably stratified vertical temperature profile and a relatively fixed core region. The intensity of convection was shown to be much smaller than in the case L/H = 1.

The specifics of heat transport in long layers were considered in [5-8], and asymptotic solutions were given for the limiting case $H/L \to 0$; in [8] the effect of boundary conditions on the upper horizontal surface on the temperature and flow structure inside a cavity were considered. A numerical study for $70 \leq Ra \leq 1.4 \cdot 10^5$, Pr = 7, $1 \leq L/H \leq 20$ was presented in [6] and an experimental study in the ranges $1.3 \cdot 10^6 \leq Ra \leq 1.1 \cdot 10^8$, L/H = 50 and 100 was discussed in [7] for water.

In [9], generalizing the experimental study of convection in a horizontal layer heated from the sides (water, $L/H = 18.2 \cdot 10^8 < Ra < 2 \cdot 10^9$), the presence of a weak counterflow between the core region and the boundary layer at the horizontal wall was demonstrated. Experimental data on the flow structure in rectangular closed cavities with $Pr \geq 10$, $10^3 \leq Ra \leq 10^7$ was obtained in [10], and the value of the critical Reynolds number, giving the onset of secondary turbulence near the vertical walls, was measured. A numerical parametric study of convective heat exchange in shallow closed cavities for $0.01 \leq Pr \leq 100$, $Ra \leq 6 \cdot 10^6$, $1 \leq L/H \leq 40$ was presented in [11]. In [12] the range (L/H = 5 and 10, Pr = 1, $10^6 \leq Ra \leq 3 \cdot 10^9$) was studied theoretically and numerically for convective flow in a horizontal cavity at large Rayleigh numbers Ra and large length ratios L/H. A 31 × 37 net was used for the numerical computations. A numerical study of the effect of thermal and concentration convection on the flow structure and on the temperature and impurity distributions was presented in [13] for the growing of a single crystal from a gas with boundary conditions of the first and second kinds with respect to temperature on the horizontal surfaces ($L/H \leq 4.4$, $Ra < 1.6 \cdot 10^4$, Pr = 0.73).

However, there has not yet been done a numerical calculation of the temperature distribution and flow structure that agrees in detail (local characteristics) with experiment at Rayleigh numbers up to 10^9 and large length-to-width ratios (up to 10-13). This is the range met with in practical applications.

The purpose of the present paper is to obtain and compare numerical and experimental data under controlled conditions in the range $10^5 < Ra < 10^9$, $6.9 \leq L/H \leq 12.7$ for a layer with adiabatic horizontal boundaries.

2. Mathematical Model and Method of Solution. The boundary-value problem under consideration is schematically shown in Fig. 1. A mathematical model of the convection is based on the two-dimensional nonsteady Navier–Stokes equations in the Bousinessq approximation [14]. Using the dimensionless velocity ω, stream function ψ, and temperature Θ as variables, we have

$$\omega_t + u\omega_x + v\omega_y = \omega_{xx} + \omega_{yy} + \mathrm{Gr}\Theta_x, \tag{2.1}$$

$$\psi_{xx} + \psi_{yy} = -\omega, \quad \Theta_t + u\Theta_x + v\Theta_y = \frac{1}{\mathrm{Pr}}(\Theta_{xx} + \Theta_{yy}),$$

$$u = \psi_y, \quad v = -\psi_x, \quad \Theta = \frac{T - T_1}{T_2 - T_1}, \quad \mathrm{Gr} = \frac{g\beta H^3 (T_2 - T_1)}{\nu^2}, \quad \mathrm{Pr} = \frac{\nu}{a}.$$

where Gr is the Grashof number; Pr, Prandtl number; Ra = GrPr, Rayleigh number; ν, a, β, kinematic viscosity, thermal conductivity, and thermal expansion coefficient, respectively. In the calculations ν, a, β were taken as constants evaluated at the mean temperature $(T_1 + T_2)/2$. The scales of length, time, velocity, and temperature were chosen as H, H^2/ν, ν/H, $\Delta T = T_2 - T_1$.

The conditions $\psi = 0$, $\partial\psi/\partial n = 0$ are specified for the velocity field along the entire boundary, where n is the normal to the surface. The boundary conditions for the temperature field have the form

$$x = 0,\ 0 \leqslant y \leqslant 1,\ \Theta = 0,$$
$$x = L/H,\ 0 \leqslant y \leqslant 1,\ \Theta = 1, \tag{2.2}$$
$$0 < x < L/H,\ y = 0,\ y = 1,\ \partial\Theta/\partial y = 0.$$

The initial conditions are

$$\psi = 0,\ \omega = 0,\ \Theta = x/L. \tag{2.3}$$

Equations (2.1)-(2.3) were solved by the method of finite differences following [15], which is based on the implicit use of the monotonic approximation [16]. The boundary conditions on the stream and vortex functions are approximated by the method of [17]. We used the set of programs for the numerical solution of the unsteady Navier–Stokes equations developed in the Institute of Mechanics Problems, Academy of Sciences of the USSR [15]. The computations were done on a net uniform along the y axis (the number of points was either 33 or 65) and nonuniform along the x axis (the smallest step size, $h_{min} = 5 \cdot 10^{-3}$, was at the walls).

The difficulty in choosing the right net is that at large length-to-width ratios and large Rayleigh numbers one simultaneously requires a description of the flow structure in the core region and also in an extremely thin boundary layer at the lateral boundaries. Therefore, the net must be detailed (with many points), but, on the other hand, the number of points is limited by a rapid increase in the amount of computer time required. For example, the time required for a single run on a 141 × 33 net (on a computer of the type EC-1055) was about 12 h, on average. We point out that calculations done on a net that is too rough (e.g., see [12]) may not show some of the fine details of the flow structure discussed below.

3. Experimental Study. The setup for the experiment included a rectangular tub measuring 150 × 150 × 900 mm. The lateral walls of the tub were thermally insulated by using double slides of organic glass (10 × 150 × 920 mm) with an air interlayer for the front (transparent) wall, and a foam filler of thickness 15 mm between the slides for the back wall. The lower horizontal base was an organic glass plate of thickness 3 mm. Between the base of the tub and the foam support (90 × 170 × 1000 mm) was placed a foam plate (15 × 170 × 1000 mm).

The upper horizontal plate was made of two organic glass plates (3 × 145 × 810 mm) with a foam-filled cavity between them (15 × 125 × 790 mm). The horizontal thermally insulated plate of length x_0 = 810 mm had a transparent slit (δ = 5 mm) along its entire length at distances z = 45 mm and z = 75 mm from the front face.

Heat exchange along the vertical faces of the tub was established by making each of them from brass plates (10 × 148 × 148 mm) and organic plates with a cavity (20 × 130 × 130 mm) between the two plates. The constancy of the temperature on the heat-exchange surfaces was insured by circulation of thermostatically controlled water inside the cavity. The thermostat SZhML-19/2.5 was used, which maintained a temperature constant to ±0.03°C. Measurement of the temperature of each heat-exchange surface was done with two Nichrome–Constantan alloy thermocouples made of 0.1-mm-diameter wires. The thermocouple was mounted inside a cylinder of diameter d = 0.8 mm and could be placed inside a face-drilling of d = 1 mm at different heights at a distance 0.5 mm from the heat-exchange surface. The thickness of the water layer was determined with the help of calibrated plates on which the upper horizontal plate was placed. In the case of two rigid bounding surfaces, the liquid touched the upper of the two plates. A free surface was created by filling the tub to the necessary height without touching the upper plate. The distance between the liquid free surface and the thermally insulated upper plate was 5-7 mm. The alignment of the tub to true horizontal was done by adjusting screws and was monitored with the cathetometer KM-8 to within 0.01 mm.

The temperature of the liquid layer was measured using a thermocouple probe of two Constantan–alloy thermocouples made of 0.1-mm-diameter wires. The Γ-shaped probe was inserted through a 5-mm gap between the back wall of the tub and the face of the upper horizontal plate. The thermocouples were aligned one above the other with the upper one close to the upper wall,

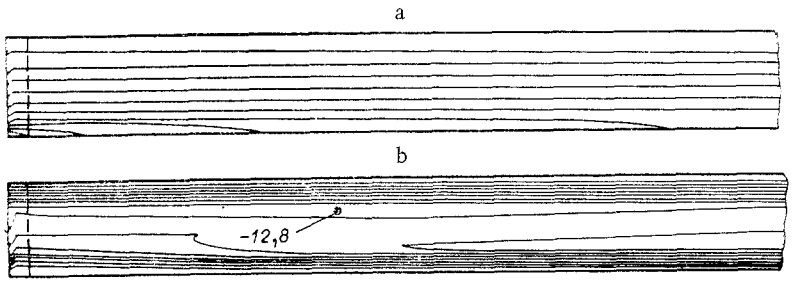
a
b
-12,8

Fig. 2

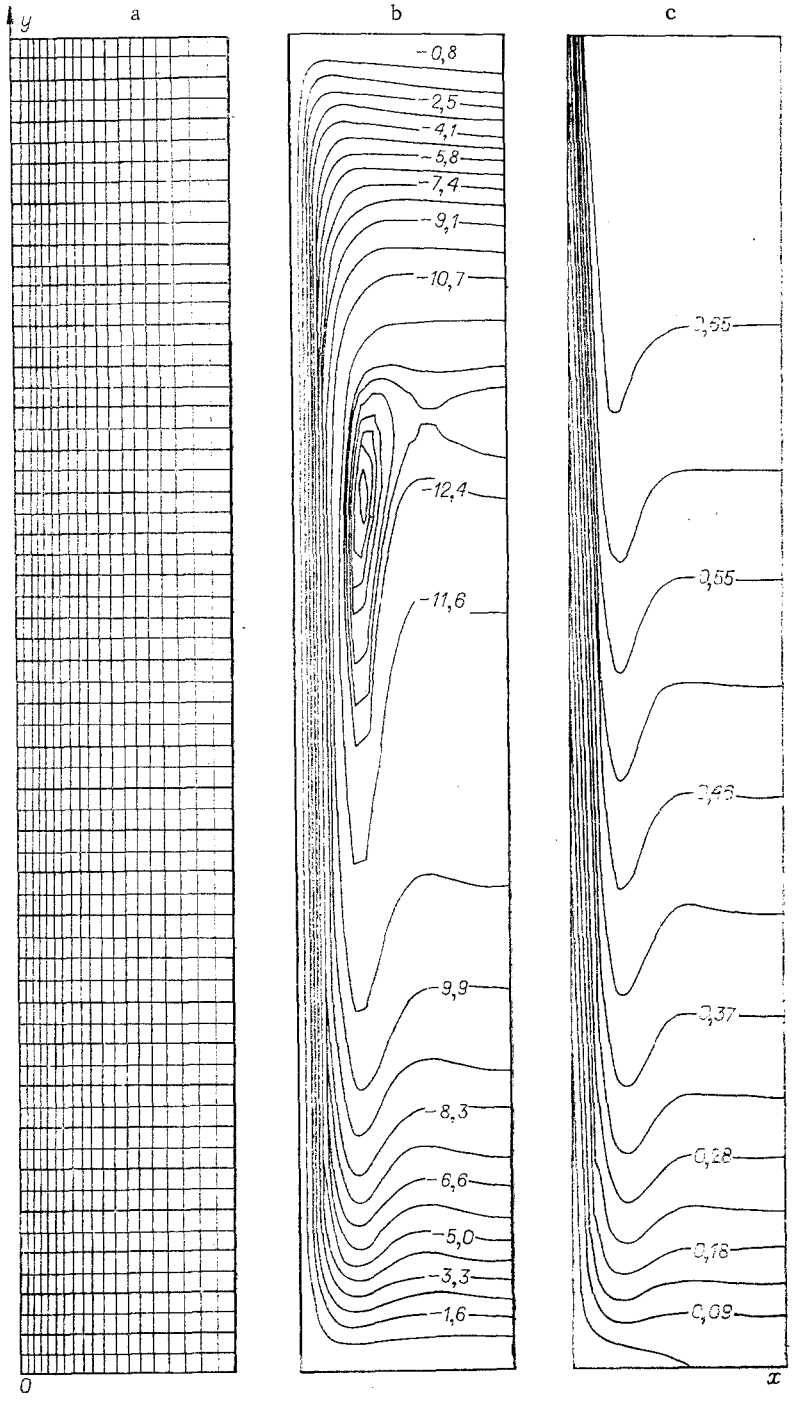
y
a
b
c
-0,8
-2,5
-4,1
-5,8
-7,4
-9,1
-10,7
-12,4
-11,6
-9,9
-8,3
-6,6
-5,0
-3,3
-1,6
0,55
0,37
0,28
0,18
0,09
0
x

Fig. 3

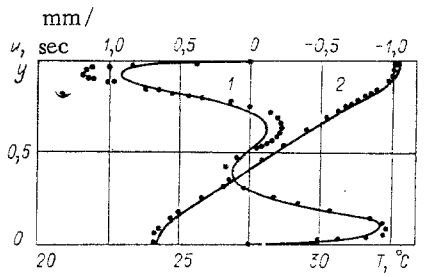

Fig. 4

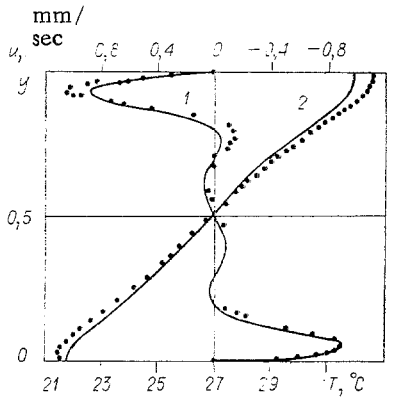

Fig. 5

and the lower one close to the lower wall. The thermocouple was movable in the vertical (y) and horizontal (x) directions, and also (by turning the probe) in the third (z) direction. The displacement of the thermocouple probe along the vertical was monitored by the cathetometer KM-8 to within 0.01 m with a coordinate spacer with 0.05-mm scale divisions. The emf of the thermocouple was measured with the digital volt–ammeter F-30.

The flow velocity of the liquid layer was measured by making the flow visible with the help of aluminum particles suspended in the liquid during the entire experiment, lasting 9-10 h. The liquid layer with its aluminum particles was transparent along its entire width z_0. The largest value of the horizontal component of the velocity did not exceed 2.5 mm/sec. Therefore, the velocity could be determined by measuring the time required for particles to pass a fixed distance on the grid of the cathetometer (KM-8) telescope. After filling the tub with liquid and installing the upper horizontal plate, the gap between this plate and the tub was thermally and materially insulated from the ambient medium such that, during the entire experiment, no noticeable evaporation of the sample liquid occurred. The experiment showed that the distilled water-free surface was fixed in space ($u_{y=H} = 0$); this was due to surface-active material in the water. Therefore, under the conditions of the experiment, the free surface of the water behaved as a rigid surface.

4. Computational and Experimental Results. For large Rayleigh numbers and large length-to-width ratios, and for the ranges of the other parameters considered in the study, extremely thin hydrodynamic and thermal boundary layers formed at the vertical and horizontal walls. Outside the vertical boundary layers, the temperature along a horizontal cross section was practically constant. The liquid, as a whole, was stably stratified with respect to the vertical, but a weak counterflow between the core region and the boundary layers was observed.

The flow structure and temperature distribution can differ significantly from the case for small and moderate Rayleigh numbers. In Fig. 2 we show the isotherms (a) and flow lines (b) for $Ra = 1.2 \cdot 10^8$, $Pr = 5.8$, $L/H = 12.7$. In Fig. 3, curves a, b, and c show the computational net, the flow lines, and the isotherms, respectively, near the left face of the layer ($0 \leq x \leq 0.16$, $0 \leq y \leq 1$); this region is shown by the dashed line in Fig. 2. The structure of the hydrodynamic and thermal boundary layers at the vertical walls can be seen from these plots. The longitudinal temperature differential is localized in very narrow vertical boundary layers; in the upper part of the thermal boundary layer near the left wall (and in the lower part near the right wall) the longitudinal temperature differential for $Ra = 1.2 \cdot 10^8$, $Pr = 5.8$ was $\sim 0.7(T_2 - T_1)$. The vertical velocities were such that a heated mass of liquid in the upper parts of the layer was not able to lose heat and moved into the cooler, lower part of the layer. Then, because of buoyancy forces, the liquid rose to a height with the same temperature. Thus, the weak counterflow near the vertical walls mentioned above arises. This is seen in Fig. 3b. At large Rayleigh numbers, this counterflow can produce a weak secondary vortex at the vertical wall, as shown in Fig. 3b. In the experiments done in [10] for $L/H \gg 1$, a critical Rayleigh number Re_* was found for the onset of this secondary vortex motion; it is given by $Ra\,(L/H)^{1/4} \sim 6.4 \cdot 10^5 \pm 10\%$.

In the computations done here, these vortices could be resolved by the net, but were small for the values of L/H and Ra used in the calculations. The vortices were near the walls, between the vertical boundary layers and core region, and were drawn along the vertical. The main part of the counterflow tilts in the direction of the core region, and forms

TABLE 1

Pr	L/H	Computational net	Ra	ψ_m	Nu
7,2	6,94	141×33	$7{,}92\cdot10^7$	8,35	28,2
5,8	6,94	141×65	$8{,}7\cdot10^7$	10,8	29,03
5,8	6,94	141×65	$5{,}8\cdot10^8$	16,04	49,50
5,8	12,7	141×65	$1{,}2\cdot10^8$	12,68	30,37

a weak horizontal flow (see Figs. 2 and 4). This horizontal counterflow was observed in the experiment of [9], but was not observed in the numerical solution of [12] because the computational net used there was too rough.

A comparison of the computational and experimental results is shown in Figs. 4 and 5 ($Ra = 1.2\cdot10^8$, Pr = 5.8, L/H = 12.7 for Fig. 4; $Ra = 5.8\cdot10^8$, Pr = 5.8, L/H = 7 for Fig. 5). The solid curves give the calculated velocity and temperature profiles along the center cross section (the points are the experimental values). Some asymmetry in the experimental data can be seen; this is probably due to the temperature dependence of the viscosity. In the calculations, the viscosity was taken as a constant evaluated at the mean temperature $(T_1 + T_2)/2$. Note that the flow is stable and steady in both the experiment and the calculations.† This is connected with the specifics of the problem (stable vertical temperature stratification, the controlled thermal conditions of the horizontal walls), and is important in choosing growth regimes of single crystals from melts, where temperature fluctuations in the melt in the stages before crystallization can lead to defects in the crystal structure (the so-called lamellar inhomogeneity [18]). Some of the computational results are shown in Table 1, where ψ_m is the maximum value of the stream function, $\mathrm{Nu} = \int_0^1 \frac{\partial\Theta}{\partial x}dy$ is the average value of the Nusselt number on the face x = 0.

The satisfactory agreement between the computational results and the experimental data implies that, under the conditions considered here, three-dimensional effects are apparently not significant.

The results of our study on the flow structure and temperature distribution near the vertical boundaries are of interest in questions of the morphological stability of a crystallization front. In particular, the results show that the hydrodynamics in the region near the front is very complex for the ranges of parameters of interest in technology, and specialized methods are necessary for monitoring and controlling these flows.

LITERATURE CITED

1. G. Z. Gershuni, E. M. Zhukhovitskii, and V. M. Myznikov, "On the stability of plane-parallel flow in a horizontal liquid layer," Zh. Prikl. Mekh. Tekh. Fiz., No. 1 (1974).
2. G. Z. Gershuni, E. M. Zhukhovitskii, and E. L. Tarunin, "Numerical study of steady convection in a rectangular cavity with free boundaries," Acad. Notes, Permsk Univ. Gidrodinamika, Issue 3 (1971).
3. V. I. Polezhaev, "Flow and heat transport in laminar natural convection in a vertical layer," in: Heat and Mass Transfer, Vol. 1. Heat and Mass Transfer in Bodies Interacting with Liquid and Gas Flows [in Russian], Energiya, Moscow (1968).
4. V. D. Zimin, Yu. N. Lyakhov, and G. F. Shaidurov, "Experimental study of the temperature field in natural convection of a fluid in a closed rectangular cavity," Acad. Notes, Permsk Univ., Gidrodinamika, Issue 3 (1971).
5. D. E. Cormack, L. G. Leal, and J. Imberger, "Natural convection in a shallow cavity with differentially heated end walls. Part 1: Asymptotic theory," J. Fluid Mech., 65, Pt. 2 (1974).
6. D. E. Cormack, L. G. Leal, and J. H. Seinfeld, "Natural convection in a shallow cavity with differentially heated end walls. Part 2: Numerical solutions," J. Fluid Mech., 65, Pt. 2 (1974).

†This is true only for the values of the Prandtl number considered here.

7. J. Imberger, "Natural convection in a shallow cavity with differentially heated end walls. Part 3: Experimental results," J. Fluid Mech., 65, Pt. 2 (1974).
8. D. E. Cormack, G. P. Stone, and L. G. Leal, "The effect of upper surface conditions on convection in a shallow cavity with differentially heated end walls," Int. J. Heat Mass Transfer, 18, 635 (1975).
9. A. Bejan, A. A. Al-Homoud, and J. Imberger, "Experimental study of high-Rayleigh-number convection in a horizontal cavity with different end temperatures," J. Fluid Mech., 109, 283 (1981).
10. P. G. Simkins and T. D. Dudderar, "Convection in rectangular cavities with differentially heated end walls," J. Fluid Mech., 110, 433 (1981).
11. G. Shiralker and C. L. Tien, "Numerical study of laminar free convectiion in shallow closed cavities," Teploperedacha, No. 2 (1981).
12. G. Shiralker, A. Gadgil, and C. L. Tien, "High Rayleigh number convection in shallow enclosures with different end temperatures," Int. J. Heat Mass Transfer, 24, No. 10 (1981).
13. J. C. Launay, J. Miroglio, and B. Roux, "Contributions to the study of natural convection in a sealed tube for the growing of a single crystal by gas phase transport," J. Cryst. Growth, 51, 61 (1981).
14. L. D. Landau and E. M. Lifshits, Mechanics of Continuous Media [in Russian], GITTL, Moscow (1954).
15. A. V. Bune, V. L. Gryaznov, K. G. Dubovik, and V. I. Polezhaev, "Methods and computer programs for the numerical modeling of hydrodynamical processes by the nonstationary Navier–Stokes equations," Preprint No. 173, IPM, Academy of Sciences of the USSR (1981).
16. A. A. Samarskii, Theory of Differences [in Russian], Nauka, Moscow (1977).
17. V. I. Polezhaev and V. L. Gryaznov, "Method of calculating boundary conditions for the Navier–Stokes equations in terms of the vorticity and stream function variables," Dokl. Akad. Nauk SSSR, 219, No. 2 (1974).
18. R. A. Lodiz and R. L. Parker, Growth of Single Crystals [Russian translation], Mir, Moscow (1974).

LONGITUDINAL CELLULAR STRUCTURES OF TAYLOR–GÖRTLER TYPE VORTICES ON THE HIGH-PRESSURE SIDE OF ROTATING CHANNELS

L. V. Kuz'minskii, E. M. Smirnov, and S. V. Yurkin

UDC 532.516

The linear stability of Poiseuille flow between two plates rotating about an axis parallel to the plates and normal to the direction of the basic flow was studied in [1, 2]. It was shown that the flow is least stable to disturbances in the form of standing waves, known as Taylor–Görtler vortices. The results of the experimental determination of the region of flow parameters for the formation of above vortices are given in [1] for a channel with rectangular section, strongly stretched along the axis of rotation. Experimental results agree well with linear theory. At the same time, it remains unclear about the important question of the effect of side walls on the stability of the basic flow in practically interesting cases of channels with moderate aspect ratio and, in particular, in channels with square cross section. The problem is formulated below and the results of experimental study of this problem are discussed.

The restructuring of the basic flow due to rotation was studied analytically and numerically in [3-6], assuming developed flow in rectangular cross-sectional channel. Here, as usual, developed flow means that the flow is sufficiently far from the entrance where the initial conditions are completely "forgotten" and the flow characteristics are identical at all cross sections.

As characteristic parameters for the channel with the given aspect ratio $\kappa = h/l$ we choose Reynolds number $Re = w_m l/\nu$ and the rotation parameter $K = \omega l/w_m$, where h and l are the

Leningrad. Translated from Zhurnal Prikladnoi Mekhaniki i Tekhnicheskoi Fiziki, No. 6, pp. 129-134, November-December, 1983. Original article submitted October 13, 1982.

 0021-8944/83/2406-0882$07.50 © 1984 Plenum Publishing Corporation